Apo structure of the ligand-binding domain of aspartate receptor from *Escherichia coli* and its comparison with ligand-bound or pseudoligand-bound structures

Young-In Chi, Hisao Yokota, Sung-Hou Kim*

Department of Chemistry and Lawrence Berkeley National Laboratory, University of California, Berkeley, CA 94720, USA

Received 2 June 1997; revised version received 18 July 1997

Abstract The aspartate receptor from *E. coli* is a dimeric transmembrane-signaling protein that mediates chemotaxis behavior and is the most studied system among the chemotaxis receptors to understand the molecular mechanism for transmembrane signaling. However, there is an unresolved issue for the structural event which initiates the transmembrane signal upon binding to the ligand. Biochemical and genetic evidence implies an intrasubunit mechanism (monomeric model) whereas crystallographic evidence implies an intersubunit mechanism (dimeric model). Crystallographic evidence has been ambiguous because all the apo protein structures contained a pseudoligand sulfate, and a completely ligand-free structure has not been available thus far. Here we present the crystal structure of the ligand binding domain of the aspartate receptor free of the ligand aspartate or pseudoligand sulfate. The structural comparison of this structure with those of ligand-bound and pseudoligand-bound forms revealed that, on ligand or pseudoligand binding, the conformational change in the ligand-binding domain is relatively small, but there is a considerable rotation between two subunits, supporting the dimeric model.

Key words: Aspartate receptor; Transmembrane signaling; Chemotaxis; X-ray crystallography; Crystal structure

1. Introduction

The aspartate receptor is a chemotaxis receptor in which, upon binding to an attractant or a repellent, a signal is transmitted to the cytoplasm to modulate the autophosphorylation rate of a bound histidine kinase, CheA which, in turn, phosphorylates CheY, a key protein controlling the rotation of flagella motor. This receptor is composed of three functional domains: a ligand-binding (periplasmic), a transmembrane, and a signaling (cytoplasmic) domain. Among these, only the ligand-binding domain has succumbed to structure determination efforts [1–4]. Many other extracellular signal receptors such as cytokines and insulin receptors have similar domain composition and are believed to share a common mechanism of transmembrane signaling. However, unlike many growth hormone receptors [5], dimerization is not sufficient for the signal transduction in the aspartate receptor because this receptor stays as a dimer in the presence or absence of aspartate [6], and disulfide-cross-linked dimers mediate near normal response to aspartate [7]. A conformational change and/or displacement of subunits within a preexisting dimeric structure is necessary for the signal transduction of this receptor, and a number of possible mechanisms accompanying these alterations have been proposed which could be classified as the monomeric model or the dimeric models (Fig. 1).

Biochemical studies such as cross-linked hybrid studies [8,9] and genetic studies [10,11] suggest that a single monomer in the dimeric receptor is sufficient to carry out aspartate-dependent signaling as measured by methylation rate of the signaling domain or aspartate-sensing ability assay of the mutant cells. These findings and the structural analogy with the *trp* repressor whose ligand-bound and ligand-free structures showed vertical displacement of the α-helices within a single monomer (see the discussions for the details) have led Lynch and Koshland Jr. [12] to propose a detailed structural model for a monomeric mechanism in which ligand binding triggers a shift in the relative position of the two transmembrane helices within a single subunit like a piston as the primary event to initiate the signal transduction.

On the other hand, crystallographic evidence supports a dimeric model. The structures of the dimeric ligand-binding domain of the *Salmonella typhimurium* aspartate receptor in 'apo' (actually pseudoligand sulfate-bound) and aspartate-bound forms showed no asymmetric translation of the helices within monomers normal to the membrane, but rather showed a small, but significant rotation of about 4° between monomers about the axis parallel to the membrane [1–3]. The result led us to propose the dimeric model in which the monomers act like scissors [1,13], or unwinders of supercoiled helices [13] as the primary event to initiate the signal transduction. This structural evidence was reconfirmed when another apo (also pseudoligand sulfate-bound) ligand-binding domain of the *E. coli* aspartate receptor was solved [4].

However, the weakness of the crystallographic evidence has been that the previous apo structures all contained sulfate ions, which were found to be bound in the ligand-binding pocket, acting as a pseudoligand. Thus, Lynch and Koshland Jr. [12] assumed that they do not represent the real apo structures and the absence of such proper conformational change proposed for the monomeric model in the crystallographic studies could be attributed to this fact.

During our attempt to crystallize the complex of the ligand-binding domain of the aspartate receptor from *E. coli* and a different ligand, maltose binding protein (MBP), in the presence of maltose, we accidentally obtained the crystals containing only the ligand-binding domain of the aspartate receptor. These crystals were grown in a condition completely free of either the ligand aspartate or pseudoligand sulfate ions (see the materials and methods for the crystallization condition), thus representing the true apo form.

The crystal structure was solved at 2.3 Å by the molecular

*Corresponding author. Fax: 1 (510) 4865272.
Email: shkim@LBL.gov

PII S0014-5793(97)01027-2

replacement method using the monomer structure grown under high sulfate ion concentration as a model, and refined to an R-factor of 18.6%. This dimer of four α-helical bundle subunits (Fig. 2) exhibits identical conformation with the previously determined aspartate-bound structures especially at the ligand-binding pocket; however, it displays a larger (8.3°) intersubunit rotation between two monomers when both structures are compared. A translational movement of the transmembrane helices within the monomers was not observed between these two structures. These findings in conjunction with earlier structural studies of the cross-linked mutant of ligand-binding domain from *Salmonella* with aspartate or sulfate [1], the wild-type domain from *Salmonella* with aspartate or sulfate [2,3], and the wild-type domain from *E. coli* with sulfate [4] provides supporting evidence that the dimeric model prevails over the monomeric model for the molecular mechanism of transmembrane signaling in the bacterial aspartate receptor.

2. Materials and methods

2.1. Protein preparation and crystallization

In an attempt to crystallize the complex of the intact MBP and the ligand-binding domain (residues 37–180) of the *E. coli* aspartate receptor, both proteins were produced by similar procedures described for the previous structures [1,14]. The intact MBP protein was purified by running an amylose column whereas the ligand-binding domain of the aspartate receptor was purified by running a Q-Sepharose column followed by a Superdex G-75 column. The purity of both samples were analyzed by mass spectroscopy and were highly pure without any modifications or heterogeneity (results not shown). The purified samples were then mixed in 10mM Hepes (pH = 7.0) buffer in various MBP:receptor ratios in the presence of about 100 fold of maltose. The sparse matrix method [15] was used to sample variety of crystallization conditions. The initial crystals were obtained by vapor diffusion method in a drop made of 1:1 (v/v) mixture of the 15 mg/ml protein solution and the mother liquor containing 4.3M Sodium chloride in 100mM Hepes buffer (pH = 7.5). Better crystals were obtained using Tris-HCl buffer (pH = 8.0) instead of Hepes buffer. The crystals belong to a space group $C222_1$ with a = 71.6Å, b = 78.6Å, and c = 52.8Å. Crystal content analysis and rotation search with various models revealed that the crystals contain only one ligand-binding domain of the aspartate receptor per asymmetric unit despite the mixed protein samples with a 1MBP:2receptor ratio.

2.2. Data collection

The native data set was collected at the beam line 1–5A at the Stanford Synchrotron Radiation Light (SSRL). The crystals were transferred to the mother liquor containing 20%(v/v) glycerol stepwise before being flash-frozen by liquid nitrogen stream at 100°K for data collection. The shorter wavelength (1.0703Å) was used to obtain a better signal to noise ratio from a small crystal. The data set was processed with DENZO [16] and scaled with CCP4 program suite [17]. The Rsym value for the data set was 9.1% with overall 5.7 times of redundancy up to 2.3Å (77.6% complete at the highest resolution shell).

2.3. Structure determination

The structure was solved by the molecular replacement method using AMORE program [18]. The coordinates of the ligand-binding domain of the aspartate receptor from *E. coli* (4) were obtained from the Protein Data Bank and used as the search model. We used the entire model (residues 38 to 179) without any modification. The search was carried out with the data between 15.0 and 3.0 Å, and center of mass cutoff as 20 Å. The best solution which stood out well above the next possible solution (32% higher in correlation coefficient) had a correlation coefficient of 61.8%, and an R-factor of 40.6%. The subsequent refinement of each helices as a rigid body using X-PLOR [19] reduced the R-factor from 42.0% to 40.2% between 8.0 and 2.3 Å data.

2.4. Model refinement

Throughout the refinement, the R_{free} value [20] was monitored to check the real progress. Initial positional refinement of the rigid body-refined model using 8.0–2.3Å data followed by group B-factor refinement dropped the R_{free} to 38.6%. The refinement was then continued with the simulated-annealing protocols implemented in X-PLOR 3.1 [19]. Restraints were placed on bond lengths, bond angles, non-bonded contacts and temperature factors of neighboring atoms; no correction for solvent continuum was made. 2Fo-Fc maps as well as omit maps were calculated at regular intervals to allow manual rebuilding of side chains with different rotamers from the search model. Bound solvent molecules (all regarded as water) were added conservatively with due regard for their environment including potential interactions with hydrogen-bond partners. The solvent model was comprehensively checked several times during refinement by omitting all water molecules that had high B values (>60 Å^2), or made either too-close contacts with each other or with protein atoms, or made no potential hydrogen-bonded contacts at all. At the end of the refinement the crystallographic R factor was 18.6% and R_{free} value was 27.5%. The detailed refinement statistics are shown in Table 1. A representative portion of 2Fo-Fc map with the final model and Fo-Fc difference map for Arg64 and the surrounding water molecules are shown in Figs. 3A and 3B, respectively.

3. Results

3.1. Description of the structure

The overall monomer structure has the same fold as the previously determined apo (sulfate-bound) or ligand-bound structures. The dimer is made of two identical monomers that are related by a crystallographic two-fold axis. The monomer consists of four main helices, 1 (residues 38–75), 2 (residues 86–110), 3 (residues 116–142), and 4b (residues 153–180), and a short helix, 4a (residues 145–151), is found in the connection between helices 3 and 4b. A portion of the loop (residues 78–85) connecting helices 1 and 2 are not seen in the electron density map and are presumably disordered as reported in the previous structures. The helices 1 and 4 would continue towards the membrane to become the two transmembrane helices (TM1 and TM2, respectively), one of which (TM2) being connected to the cytoplasmic signaling domain.

3.2. Ligand-binding pocket

The initial attention was focused on the aspartate binding pocket between helix 1 and helix 4 because this crystal was grown in the absence of sulfate ions which occupied the lig-

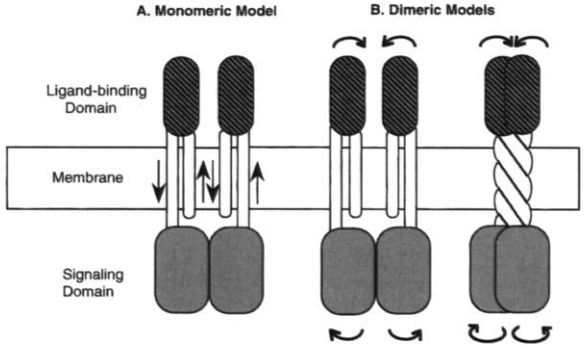

Fig. 1. Models for the mechanism of transmembrane signal transmission in the aspartate receptor. A. Monomeric model, in which ligand binding alters the relative position/orientation of the transmembrane helices within a monomer. B. Dimeric models, in which ligand binding brings two monomers closer by a slight rotation with each other like scissors or unwinders of the supercoiled transmembrane four-helix bundle resulting in a greater shift in the relative orientation of the two signaling domains.

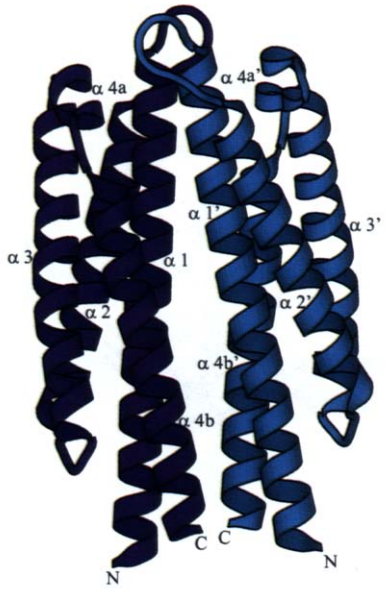

Fig. 2. Ribbon diagram of the dimeric aspartate receptor ligand-binding domain free of either the ligand aspartate or pseudoligand sulfate ions.

and-binding pocket in the previous apo structures. Contrary to what has been proposed by Lynch and Koshland Jr. [12], the translational movement of the helix 4 (TM2) with respect to the helix 1 (TM1), or any significant differences were not seen in our structure; instead, the sulfate ion was replaced by several water molecules (Fig. 3B). Arg64 is at the same position and only adopts different chi torsion angles to accommodate the new hydrogen bonding environment. There was no residual densities in the Fo-Fc map in this region which would indicate the presence of heavier non-water ions which were not accounted for.

3.3. Intersubunit rotational angles

When our structure was compared with the pseudoligand-bound structure from *E. coli*, a small rotation of the second subunit was noticed (Fig. 4) just like it was noticed when the pseudoligand-bound structure and the ligand-bound structure from *Salmonella* were compared. To measure the intersubunit rotational angles, a least-square fit superposition for one subunit was performed using the Cα atoms of the entire subunit to the equivalent subunit of the molecule under comparison, and the matrix relating the remaining subunits was calculated. Then the rotation angle information was extracted from the matrix. These calculations were done using the graphic program O [21]. We calculated those angles for three structures, each representing different ligand binding status: one with bound aspartate, one with bound sulfate, and one completely ligand-free. For the aspartate-bound form, we used one from *Salmonella* because the attempts to crystallize the aspartate-bound form from *E. coli* have been unsuccessful thus far. The sequence identity between the two is 68%. Those values shown in Table 2 clearly demonstrated that greater rotation is observed when the ligand-bound and ligand-free forms are compared. The rotation angle between the ligand-bound and pseudoligand-bound forms, or the pseudoligand-bound and ligand-free forms turned out to be intermediate values.

4. Discussion

In the monomeric model, ligand binding at the dimer interface is proposed to trigger a shift in the relative vertical position or orientation of the two transmembrane helices (sliding of TM2) within a monomer (Fig. 1A). This model became more persuasive when the structural similarities were found between the ligand binding domain of the aspartate receptor and the *trp* repressor of *E. coli* [12]. Based on the similarities, Lynch and Koshland Jr. hypothesized that the ligand-induced conformational changes similar to that found in the *trp* repressor at the active sites would occur in the aspartate receptor ligand binding domain (Fig. 5). Because the Arg84 of the *trp* repressor (corresponding to Arg64 in the aspartate receptor, Fig. 3B) swings in when the ligand is absent, interacting with adjacent residues and occupying the space vacated by absence of the ligand, a similar conformational change could occur in the aspartate receptor in its true apo state. This shift in position, in turn, makes the helix 4 (TM2) slide up or down depending on the ligand binding status and transmits the signal through the membrane like a piston.

However, this proposed swing motion of the Arg64 is not observed in our completely ligand-free structure (Fig. 3B). The entire monomer structure does not display any noticeable departure from the pseudoligand-bound structure except a rotation of one subunit with respect to the other by 3.8° (Fig. 4). This angle becomes even greater (8.3°) when the aspartate-bound structure from *Salmonella typhimurium* and our ligand-free structure are compared (see Table 2). In the dimeric models, this rotation of one ligand-binding subunit with respect to the other is proposed to be transmitted through TM2 by a scissor-like motion [1,13] or an unwinding motion of the supercoiled transmembrane four-helix bundle (Fig. 1B).

Table 1
Crystallographic refinement statistics

Resolution range	8.0–2.3 Å
R-factor	18.6%
No. of reflections used ($F > 2\sigma$)	6443
R_{free}	27.5%
No. of reflections used ($F > 2\sigma$)	310
rms bond length deviation	0.010 Å
rms angular deviation	1.274°
rms dihedral deviation	19.059°
Total no. of protein non-hydrogen atoms	1146
Total no. of water molecules	116
Average temperature factors for main chain atom only	17.53 Å^2
Average temperature factors for all atoms including waters	19.70 Å^2

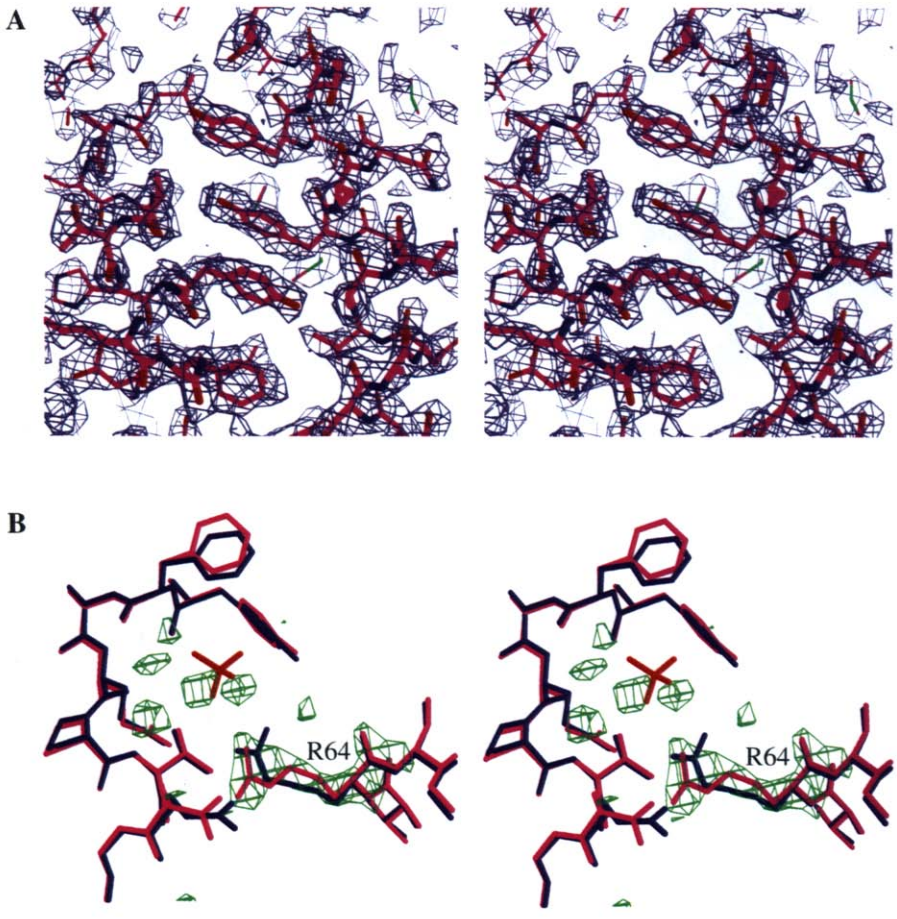

Fig. 3. A. Representative portion of 2Fo-Fc ma calculated with the final model and showing aromatic groups between helix 1 and 4b. B. Fo-Fc difference map (contoured at 3 sigma value) of one of the ligand binding pockets calculated with the model after omitting Arg64 and surrounding water molecules. The sulfate-bound form is represented with cyan (sulfate in red) and the sulfate-free form is represented with magenta. No structural differences are observed except slightly different torsion angles of Arg64 to adopt the new hydrogen bonding network by water molecules in place of the sulfate ion. Swing motion of Arg64 proposed by Lynch and Koshland Jr. [12] is not observed.

The monomer model is supported by the results of cross-linking studies [9,10], a study with partially truncated dimers [12], site-directed mutation studies [11], and ^{19}F NMR study [22]. The dimer model is consistent with all the crystallo-

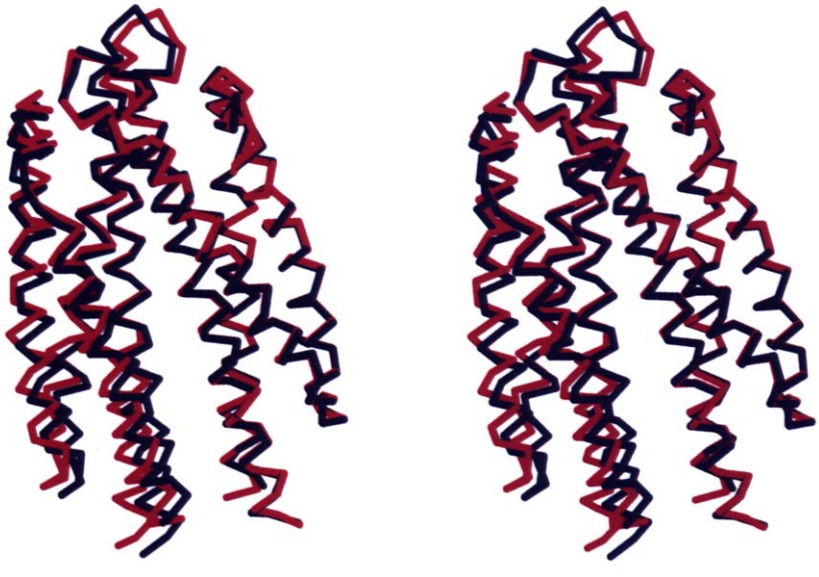

Fig. 4. Wire representation of the superimposed aspartate receptor ligand-binding domain structures with pseudoligand sulfate bound form (cyan) and ligand free form (magenta). While one subunit is very well superimposed, the other subunit is off by a small rotational angle.

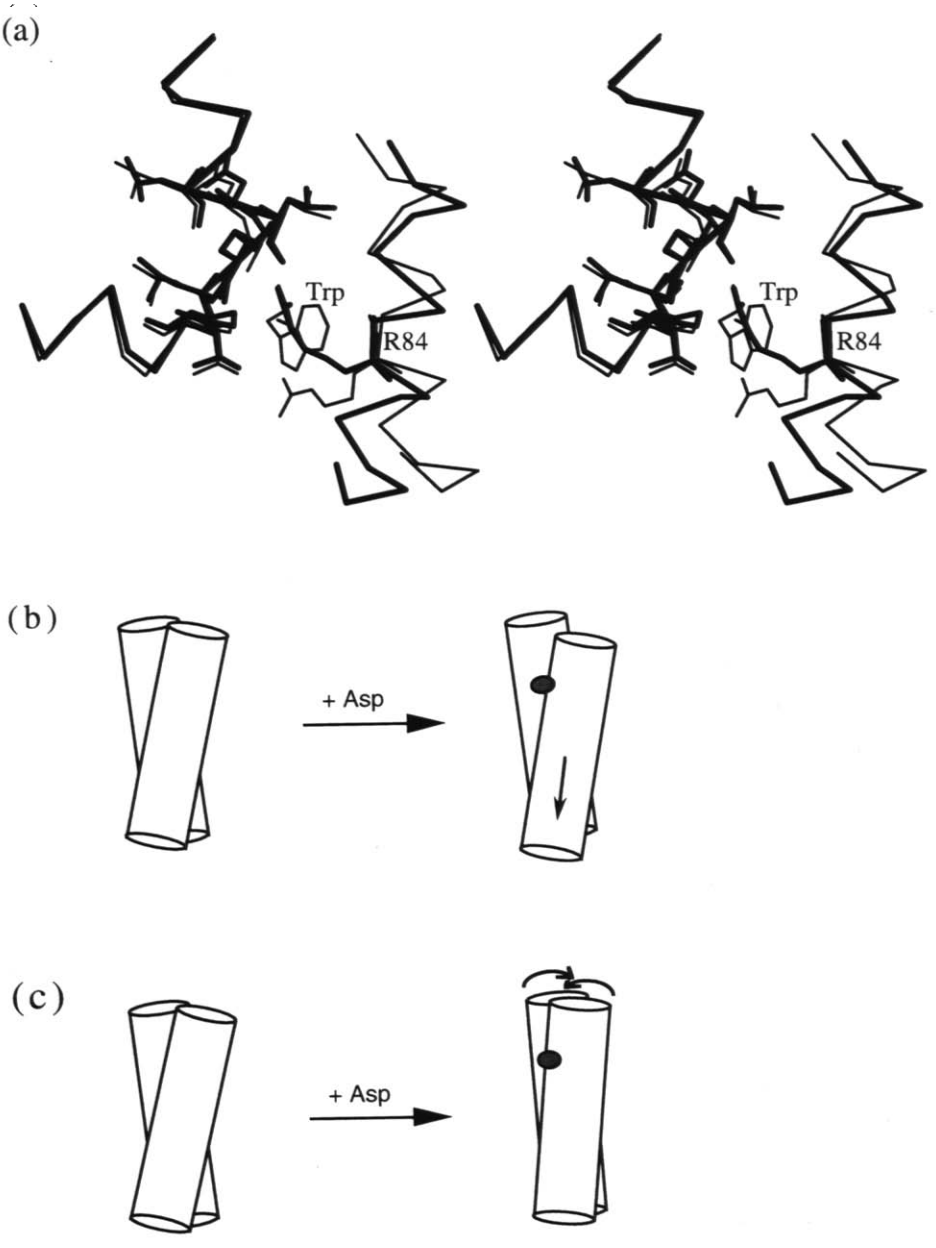

Fig. 5. A. Stereo stick representation showing the swing motion of Arg84 between the apo *trp* repressor (thick line, ref. [28]) and the ligand-bound *trp* repressor (thin line, ref. [29]). B. Schematic representation of the piston-like motion proposed by Lynch and Koshland Jr. [12]. C. Schematic representation of the motion actually observed from crystallographic structures. In the figure b and c, only helix 4 and 4′ of the dimeric receptor are shown for clarity. Aspartate binds between helix 1 and 4 of one monomer in the dimeric receptor and helix 4 continues through membrane to the cytoplasmic signaling domain.

graphic studies of the ligand domain with and without a ligand ([1–4], and this work), the studies of changes in coiled-coil interactions on aspartate receptor signaling [23,24], and a random-cassette mutagenesis study of residues at the helical faces in transmembrane segments [25].

Some variations of the above mentioned two models have

Table 2
Intersubunit rotational angles when each structures on the column and row are compared: a larger rotation angle is noticed when the aspartate-bound structure is compared with the completely ligand-free structure; a positive angle makes the dimer more compact

	Escherichia coli no sulfate ion[a]	*Escherichia coli* sulfate ion[b]	*Salmonella typhimurium* aspartate[c]
Escherichia coli no sulfate ion[a]		3.8°	8.3°
Escherichia coli sulfate ion[b]			4.9°
Salmonella typhimurium aspartate[c]			

[a]Ligand-free *E. coli* aspartate receptor structure (our presenting structure).
[b]Pseudoligand-bound *E. coli* aspartate receptor structure [4].
[c]Ligand-bound *Salmonella typhimurium* aspartate receptor structure [1–3].

been proposed [26,27], but the essence of the differences in all the models remains to be whether signaling is transmitted by the conformational changes within individual monomer or between two monomers in a dimer.

The biochemical and genetic evidence [8–11] which were interpreted to support the monomer model do not rule out the possibility of the dimeric mechanisms. In these experiments the dimeric receptors containing only one functional signaling domain were used to show that they could initiate aspartate-dependent signaling. Since dimerization of the ligand binding domain is still required for ligand binding, the scissoring or unwinding of transmembrane helices initiated by the rotation of two ligand domains might be necessary to achieve a proper positioning of the cytoplasmic signaling domain with respect to the membrane surface and resultant conformation of the monomeric signaling domain due to its new positioning for the proper signal. One possibility is that the previously buried residues of the signaling domain near the membrane could be exposed by these motions proposed in the dimeric model, which allows CheW monomers to bind and make the ternary complex with CheA. A larger degree of rotation of each signaling domain could be made when we consider the flexible nature of long continuous helices comprising an entire transmembrane domain, and parts of ligand-binding and signaling domains.

In summary, the previously proposed monomeric model for the signaling mechanism is inconsistent is with the crystallographic results of a true apo structure described here and other liganded structures. Since dimeric models are consistent with all the crystallographic results and can not be completely ruled out by the biochemical and genetic studies, we suggest that the intersubunit rotation of the dimer is more likely mechanism for transmembrane signaling. The resolution of this issue may be more clearly obtained from the three-dimensional structures of the entire intact receptor with and without the ligand; however, the attempts to crystallize the intact receptor have not been successful thus far.

Acknowledgements: We would like to thank Chan-Kyu Park of Korea Advanced Institute of Science and Technology for a gift of the *E. coli* aspartate receptor (Tar) clone and Joanne Yeh for construction of the MBP clone and contribution to the purification of MBP. We also would like to thank Rosalind Kim for valuable discussions and Edward Berry for assistance with data collection. This work was supported by the U.S. Department of Energy (DE-AC03-76SF00098), Korea Research Institute of Science and Biotechnology, and Asahi Chemical Industry, Inc.

References

[1] Milburn, M., Prive, G., Milligan, D., Scott, W., Yeh, J., Jancarik, J., Koshland Jr., D.E. and Kim, S.-H. (1991) Science 254, 1342–1347.
[2] Yeh, J., Biemann, H.-P., Pandit, J., Koshland Jr., D.E. and Kim, S.-H. (1993) J. Biol. Chem. 268, 9787–9792.
[3] Scott, W., Milligan, D., Milburn, M., Prive, G., Yeh, J., Koshland Jr., D.E. and Kim, S.-H. (1993) J. Mol. Biol. 232, 555–573.
[4] Bowie, J.U., Pakula, A.A. and Simon, W.I. (1995) Acta Cryst. D51, 145–154.
[5] de Vos, A.M., Ultsch, M. and Kossiakoff, A.A. (1992) Science 255, 306–312.
[6] Milligan, D.L. and Koshland Jr., D.E. (1988) J. Biol. Chem. 263, 6268–6275.
[7] Falke, J.J. and Koshland Jr., D.E. (1987) Science 237, 1596–1600.
[8] Milligan, D.L. and Koshland Jr., D.E. (1991) Science 254, 1651–1654.
[9] Hughson, A.G. and Hazelbauer, G.L. (1996) Proc. Natl. Acad. Sci. USA 93, 11546–11551.
[10] Tatsuno, I., Homma, M., Oosawa, K. and Kawagishi, I. (1996) Science 274, 423–425.
[11] Gardina, P.J. and Manson, M.D. (1996) Science 274, 425–426.
[12] Lynch, B.A. and Koshland Jr., D.E. (1992) FEBS Lett. 307, 3–9.
[13] Kim, S.-H. (1994) Protein Sci. 3, 159–165.
[14] Jancarik, J., Scott, W.G., Milligan, D.L., Koshland Jr., D.E. and Kim, S.-H. (1991) J. Mol. Biol. 221, 31–34.
[15] Jancarik, J. and Kim, S.-H. (1991) J. Appl. Crystallogr. 24, 409–411.
[16] Ozwinowsk, Z. (1993) in Data Collection and Processing, Sawyer, L., Isaacs, N., Bailey, S. Eds. (SERC Darsberry Laboratory, Warrington, UK) pp. 56-62.
[17] CCP4: Collaborative Computational Project No. 4. Daresbury, UK (1994) Acta Cryst. D50, 760-763.
[18] Navazo, J. (1994) Acta Cryst. A50, 157–163.
[19] Brünger, A.T. (1992) X-PLOR manual version 3.1 (Yale University, New Haven, CT).
[20] Brünger, A.T. (1992) Nature 355, 472–475.
[21] Jones, T.A., Zou, J.-Y., Cowan, S.W. and Kjeldgaard, M. (1991) Acta Cryst. A47, 110–119.
[22] Danielson, M.A., Biemann, H.P., Koshland Jr., D.E. and Falkem, J.J. (1994) Biochemistry 33, 6100–6109.
[23] Cochran, A.G. and Kim, P.S. (1996) Science 271, 1113–1116.
[24] Surette, M.G. and Stock, J.B. (1996) J. Biol. Chem. 271, 17966–17973.
[25] Maruyama, I.N., Mikawa, Y.G. and Maruyama, H.I. (1995) J. Mol. Biol. 253, 530–546.
[26] Chervitz, S.A. and Falke, J.J. (1996) Proc. Natl. Acad. Sci. USA 93, 2545–2550.
[27] Scott, W.G. and Stoddard, B.L. (1994) Structure 2, 877–887.
[28] Zhang, R.-G., Joachimiak, A., Lawson, C.L., Schevitz, R.W., Otwinowski, Z. and Sigler, P.B. (1987) Nature 327, 591–597.
[29] Schevitz, R.W., Otwinowski, Z., Joachimiak, A., Lawson, C.L. and Sigler, P.B. (1985) Nature 317, 782–786.